EFFECT OF ROLLING PROCESS ON THE MICROSTRUCTURE EVOLUTION AND MECHANICAL PROPERTIES OF 9Mn STEEL*

Ning Yan [1]
Hongshuang Di [2]
Xihuai Gong [3]
Jianping Li [4]
Dianhua Zhang [5]

Abstract

In this work, we investigated the effect of the rolling process (warm-rolled or cold-rolled) on microstructure evolution and mechanical properties of 9Mn steel. After intercritical annealing at 670°C for 10min, both cold-rolled and warm-rolled microstructures are composed of ultra-fined austenite and intercritical ferrite. The austenite in warm-rolled sample includes two types of morphology, namely equiaxed and lamellar, which exhibits a wide distribution of grain-size. The incomplete recrystallization or recovery behavior of ferrite in warm-rolled and annealed sample results in higher yield strength and shorter yield point elongation. Moreover, the warm-rolled and annealed sample extends the TRIP-related work hardening over a broad strain range, resulting in a better combination of ultimate tensile strength and total elongation.

Keywords: Warm-rolled; Cold-rolled; Microstructure evolution; Mechanical properties.

[1] *Doctor, Student, State key laboratory of Rolling and Automation, Northeastern University, Shenyang, Liaoning Province, China.*
[2] *Doctor, Professor, State key laboratory of Rolling and Automation, Northeastern University, Shenyang, Liaoning Province, China.*
[3] *Master, Student, State key laboratory of Rolling and Automation, Northeastern University, Shenyang, Liaoning Province, China.*
[4] *Doctor, Professor, State key laboratory of Rolling and Automation, Northeastern University, Shenyang, Liaoning Province, China.*
[5] *Doctor, Professor, State key laboratory of Rolling and Automation, Northeastern University, Shenyang, Liaoning Province, China.*

1 INTRODUCTION

As the energy and environment issues become more prominent, the lightweight of automobiles has gradually become the theme of the development of the automotive industry. The third generation of advanced high strength steels (AHSS) has been widely studied because of its advantage of cost and superior mechanical properties 12. Medium Mn steel, as one of third-generation AHSS, is considered one of the appropriate options because that its mechanical property is close to high-Mn TWIP steels but its alloying cost is much lower. Generally, medium Mn steel contains 5-10 wt% Mn and the microstructure consists of ferrite and austenite 3. The good mechanical properties of medium Mn steel are primarily attributed to a larger fraction of retained austenite which relieves the local stress concentration, promotes uniform deformation and provides work hardening during the deformation process by the TRIP effect. Besides sufficient volume fraction, suitable mechanical stability of austenite is significantly important in TRIP-added steel 4. It has been reported that austenite with poor stability would transform rapidly, which adversely reduced ductility. In contrast, over-stable austenite would transform slowly or even not transform which adversely decreased strength 5-6. Therefore, reasonable processing and subsequent heat treatment play the key role in tailoring the stability of austenite.

In this work, warm rolling and intercritical annealing were employed to obtain wide-sized and multi-typed austenite with large range of mechanical stability. For comparison, cold rolling was also used. The microstructure evolution during warm rolling, cold rolling and finally intercritical annealing was studied systematically. The mechanical properties and corresponding work hardening behaviors were also discussed. This study aims to explore the correlation between deformation behavior and microstructural characteristic in a medium Mn steel.

2 MATERIAL AND METHODS

The chemical composition of the medium Mn steel was Fe-0.11C-8.65Mn-1.0Si-0.3Al (wt%), which was cast in a vacuum-induction furnace. The ingot was heated to 1250 °C for 2 hours, and then hot forged into billets with a dimension of $50\times50mm^2$. The billet was reheated to 1200 °C for 2 hours for homogenization and hot rolled to 4.5 mm-thickness after 5 passes, followed by water cooling to room temperature, as shown in figure 1a. In this study, two rolling processes were employed, namely warm-rolling and cold rolling. The warm rolling is as follows: The hot rolled steel plate was heated to 570 °C and isothermally held for 5 minutes, followed by rolling processing. This process (heating and rolling) was redone several times until reach the target thickness (1.4 mm), which is shown in Figure 2b. Another process (cold rolling) is detailed as followed: Before cold rolling, the hot-rolled plate was subjected to softening annealing (600 for 60 minutes). After cooling to room temperature in air, the plate was cold rolled to the same thickness as warm rolling process, as shown in figure 1c. Finally, all the plates were annealed at 670°C for 10 minutes, followed by air cooling. For convenience, we define the first processing (warm-rolling + intercritical annealing) as WIA, and another one as CIA.Uniaxial tensile tests were carried out at the speed of 2 mm/min on the WDW-50kN tensile testing machine at room temperature. The tensile samples were machined to standard dog-bone samples along the rolling direction (RD), according to ASTM-E8. The microstructural observations were investigated by field emission scanning electron microscope (FE-SEM, Ultra-55). The samples for FE-SEM were polished and etched in a 4% nital solution. The electron backscatter diffraction (EBSD) measurement was

carried out at an accelerating voltage of 15kV, an emission current of about 100□A

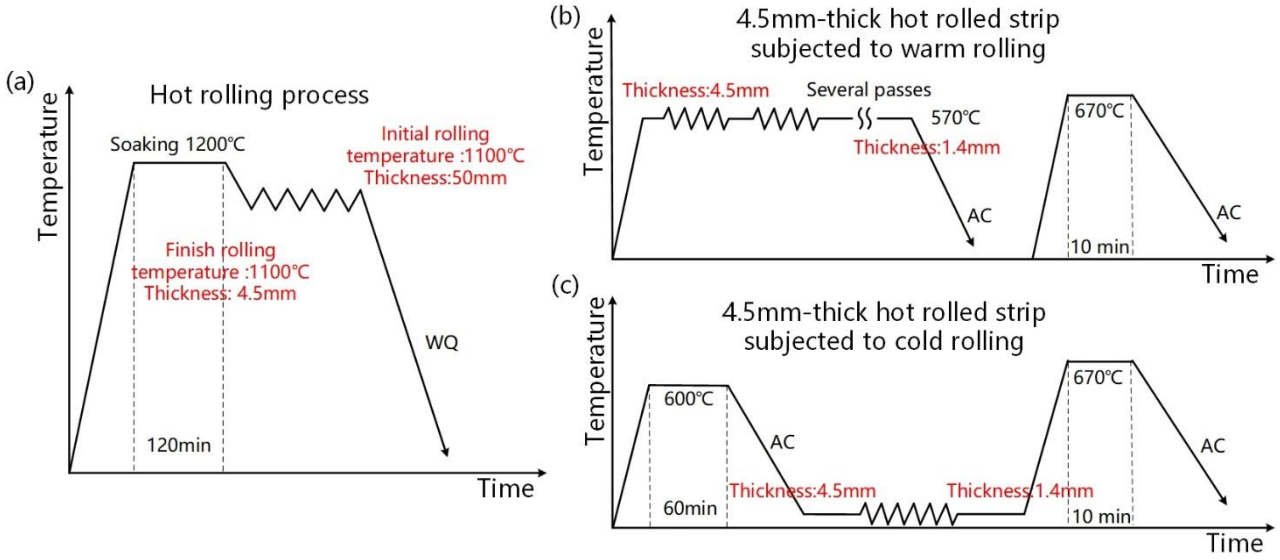

Figure 1. The illustrations of hot rolling (a), warm rolling and intercritical annealing (b), the cold rolling and intercritical annealing after hot rolling processes(c)

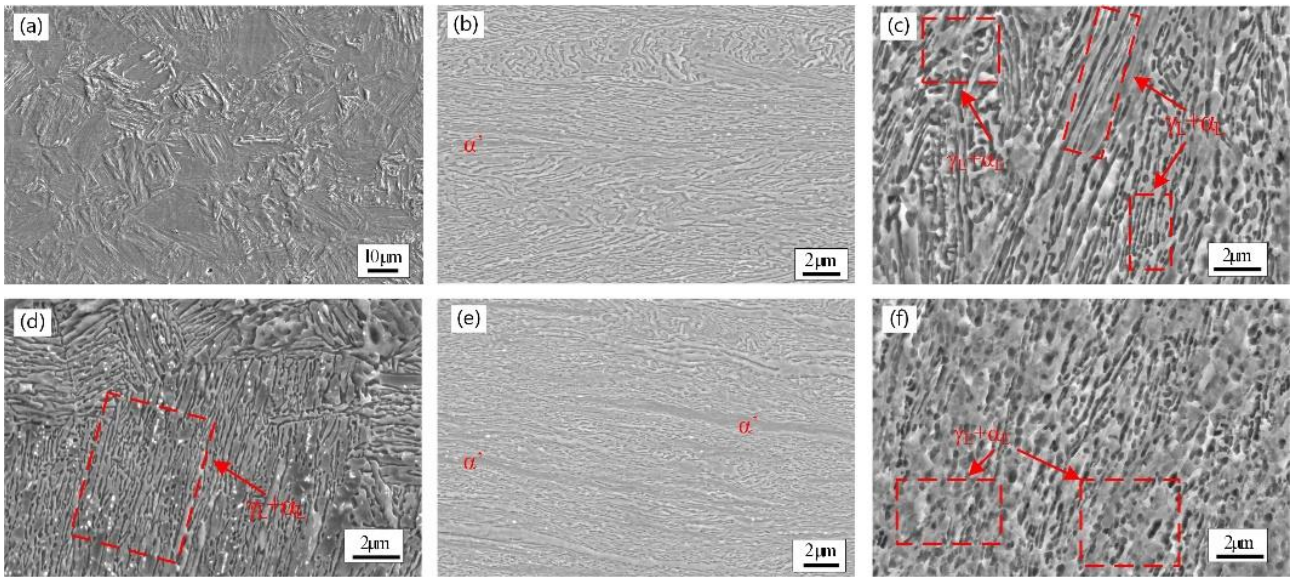

Figure 2. SEM micrographs of the microstructure of 9Mn steel obtained with the different rolling process. (a) hot rolling; (b) after warm rolling; (c) WIA; (d) softening annealing; (e) after cold rolling (f) CIA. The 'αL' and 'γL' represent lamellar ferrite and austenite; 'αE' and 'γE' represent the equiaxed ferrite and austenite; 'α'' represents martensite.

and step size of 0.03 μm. The EBSD specimens were prepared by electro-polishing using 10% perchloric acid solution. Further microstructural observation was done using transmission electron microscope (TEM), Tecnai G2 F20 performed at 200 kV. Thin foils for TEM observation were first mechanically ground to a final thickness of ~50 μm and then polished using a twin-jet polisher in a solution of 5% perchloric acid and 95% ethanol.

3 RESULTS AND DISCUSSION

3.1 Microstructure evolution

Figure 2 shows the microstructures of 9Mn steel obtained by different rolling processes. The hot-rolled microstructure contains mainly martensite and little

retained austenite (see figure 2a). After subsequent warm rolling, it is composed of deformed ferrite, austenite and some

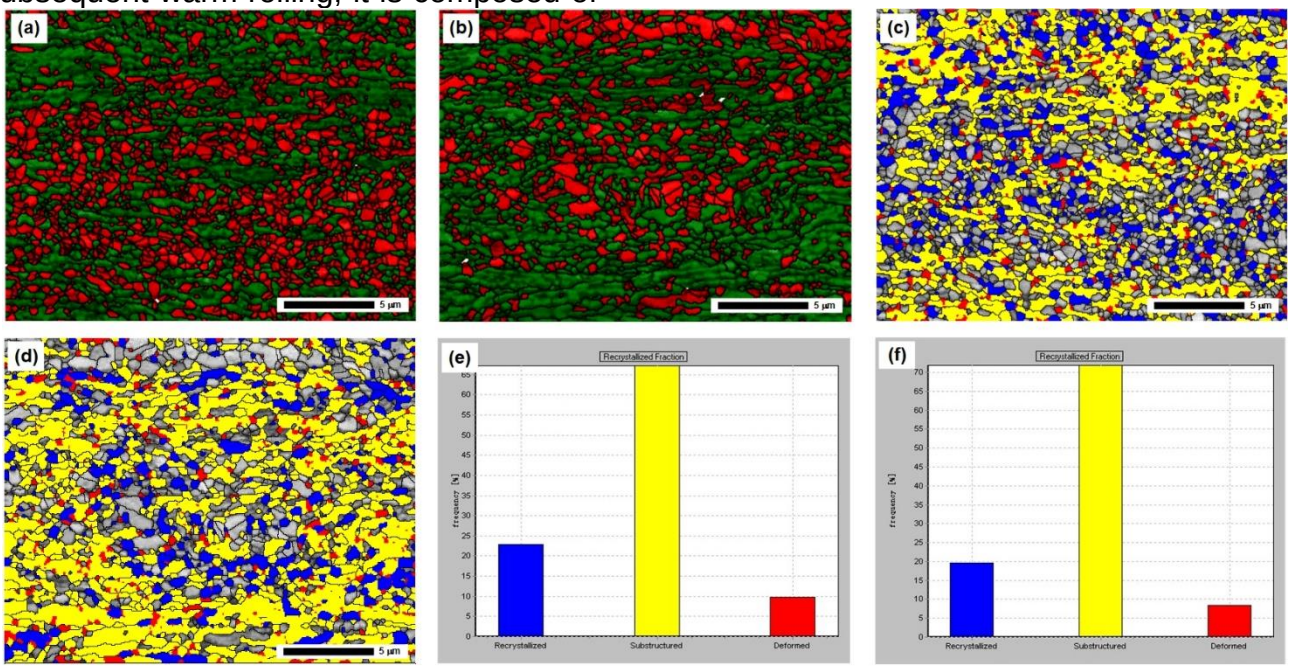

Figure 3. Microstructure after annealing and EBSD results: (a) WIA; (b) CIA; (c, d) corresponding recrystallized distribution map of (a), (b); (e, f) statistical data of recrystallization ratio in (a), (b).

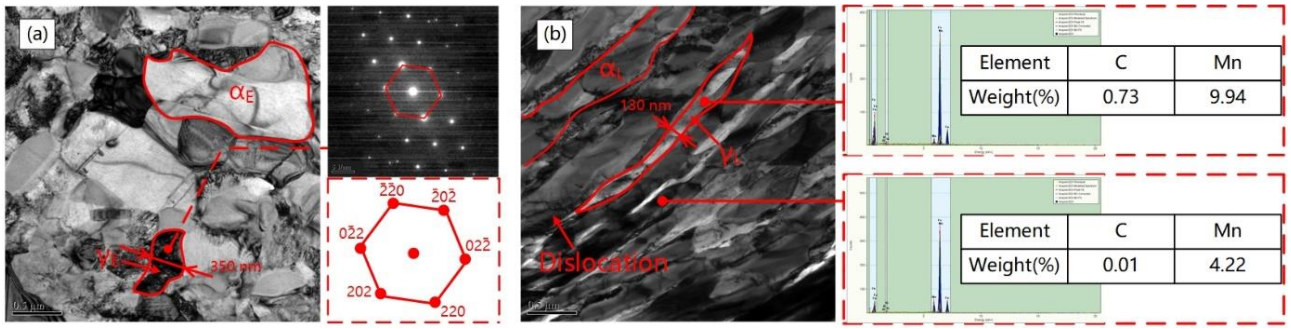

Figure 4. The transmission-electron-microscope (TEM) bright field images of WIA sample: (a) equiaxed grains and diffraction spectrum of austenite; (b) lamellar grains and EDX.

martensite that was transformed from metastable austenite. The existent of retained austenite means that there is still portioning behavior of elements (especially C and Mn) during warm rolling, even though the holding time is short (5 mins). For CIA, during softening treatment, a composed of ferrite and retained austenite. Subsequently, retained austenite is subjected to deformation during cold rolling and transformed into martensite 8, and the ferrite also undergoes serious deformation, introducing lots of dislocations. Figure 2e shows the cold rolled microstructures that consist of deformed ferrite and martensite with high dislocation density.

certain number of austenite grains were nucleated at the martensite lath boundaries and then grew to a lath-like morphology 7 (see figure 2d). Therefore, the microstructure after the first intercritical annealing was

During the succeeding IA treatment, both the deformed ferrite and martensite grains have enough stored energy and driving force to recrystallize, resulting in formation of equiaxed ferrite grains and austenite grains 910, as shown in the EBSD results in figure 3a and b. However, the difference in the deformation degree of rolling leads to different recrystallization

behavior of ferrite (figure 3c and d). According to the EBSD statistical data, figure 3e and f, the ratio of recrystallized ferrite in total BCC matrix is higher in CIA (~24%) than that in WIA (~20%). This can be attributed to the higher distortion energy

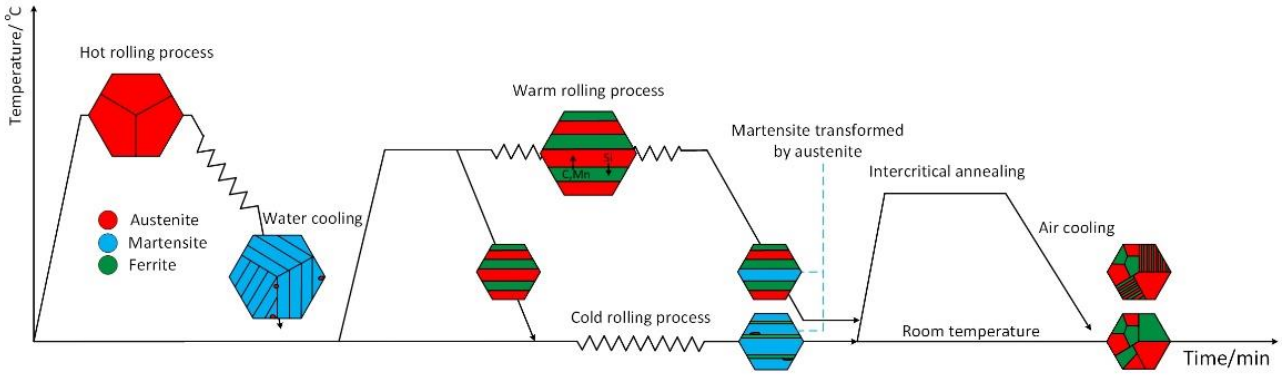

Figure 5. Microstructural evolution of medium Mn steels during rolling and annealing.

produced by deformation in the cold rolling sample, which results in a higher driving force for recrystallization. Moreover, based on the SEM observation, we also find lamellar-ferrite and lamellar-austenite, except equiaxed one. Because of the small step-size and the limit resolution of the equipment, the ultrafine lamellar-austenite is not detected by EBSD. To address this problem, field transmission scanning electron microscope with higher resolution was utilized. The results are indicated in figure 4. The lamellar-austenite with a width of ~130 nm (figure 4b) and equiaxed austenite with a diameter of ~350 nm (figure 4a) are both successfully observed. Additionally, more detailed information of ferrite is also obtained by TEM. It can be seen that there are some dislocations in lamellar ferrite, whereas equiaxed ferrite formed by recrystallization has few defects. This suggests that lamellar ferrite mainly underwent static recovery during IA rather than recrystallization, resulting in incomplete dislocation annihilating.

Moreover, the difference in ferrite recrystallization between CIA and WIA leads to various austenite growth processing. For CIA sample, the drastically deformed ferrite or martensite are prone to recrystallization during the IA, and then austenite that nucleated at the recrystallized ferrite grain boundaries would grow to an equiaxed morphology 9. On the other hand, the growth mechanism of equiaxed austenite in WIA should be the same as the CIA, while austenite that nucleated at the lamellar ferrite boundaries would grow along the boundaries resulting in lamellar morphology. Based on the above discussion, it can be concluded that the microstructural evolution of medium Mn steels during WIA and CIA processing can be well described in figure 5.

3.2 Mechanical properties

Figure 6 shows the engineering stress-strain curve and corresponding work hardening rate (WHR) of 9Mn steels after different rolling process and intercritical annealing, which exhibits excellent mechanical properties. It can be seen that the yield strength of both WIA and CIA samples exceed 900MPa. This is attributed to the ultrafine grain size of ferrite. Ultrafine grains provide a mass of grain boundaries which hinder the movement of dislocations, resulting in a great strengthening effect 11. Moreover, compared to WIA sample, the CIA sample has more recrystallized microstructure (equiaxed ferrite), see Figure 2f and Figure 3a. This recrystallized ferrite with relatively low density of dislocations is prone to deformation. Thus, CIA sample exhibits relatively low yield strength.

Figure 6b shows the work hardening behaviors of IA samples. It can be seen that both WIA and CIA samples have

similar WHR which can be divided into three stages. In 1st stage, the WHR is rapidly decreased due to dislocation dynamic recovery 12. After that, the WHRs of two samples reach a relatively low value (600 MPa) and remain flat basically at stage 2st corresponding to the yielding point elongation (YPE), namely

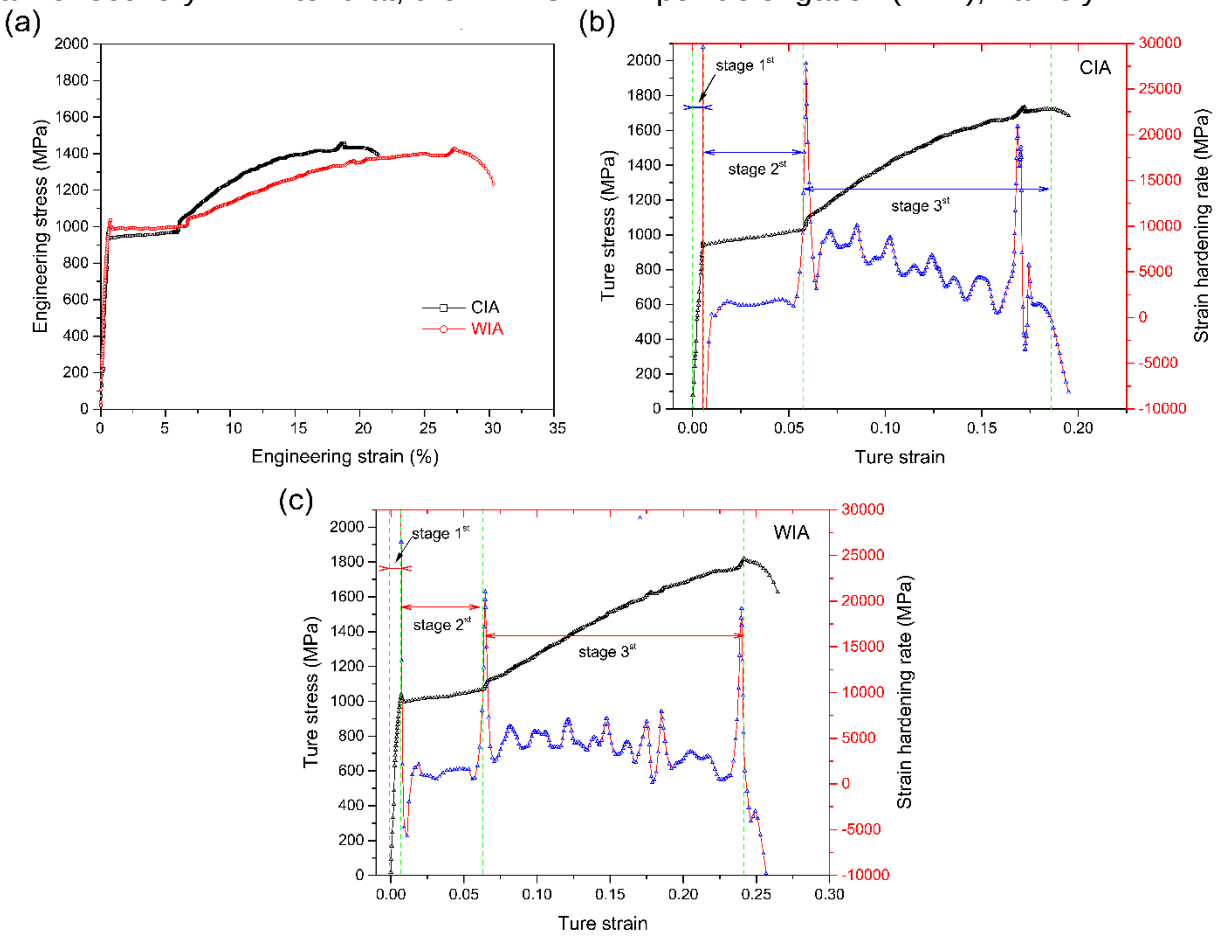

Figure 6. The engineering stress-strain curve (a) and corresponding work-hardening rate of CIA (b) and WIA (c).

Lüders strain. It has been reported that Lüders strain is associated to the interaction of mobile dislocations with dissolved carbon or nitrogen in matrix 1314. Therefore, the value of WHR reaches a relatively low level due to a large number of mobile dislocations. At the subsequent stage, the TRIP effect is activated resulting in great strain strengthening. Moreover, the work hardening behaviors of two samples are similar in this stage, significantly fluctuating with further increasing true strain. Discontinuous TRIP was suggested by Cai et al 15 to explain the serration behavior. Once certain critical stress is reached, transformation occurs continuously in the remaining austenite that has similar stability. As a result, the WHR increases rapidly followed by an abrupt drop in stress. Interestingly, for CIA sample, the total tendency of stage 3st is gradually decreased, unlike the WIA sample which is characterized by relatively flat tendency. This result can be contributed to the different mechanical stability of retained austenite between two samples. Grain size, chemical composition, and morphology of austenite 18 are considered as the key to the mechanical stability of austenite. Based on the EBSD statistical data of retained austenite grain size (see figure 7), it can be seen that the retained austenite grain sizes of two samples are sub-micron sized and have a wide size range of distribution rather than a

concentrated value, which provide the different mechanical stability, ensuring a long range of TRIP-related strain. However, this result cannot well explain the difference between work hardening behavior in stage 3st for two samples. Another point worth noting is that the difference in morphology of retained austentie between two samples. For CIA, the interaction between ferrite recrystallizaition and austenite growth result in a duplex microstructure containing recrystallized ferrite and austenite with equiaxed morphology (see figure 2 and 3).

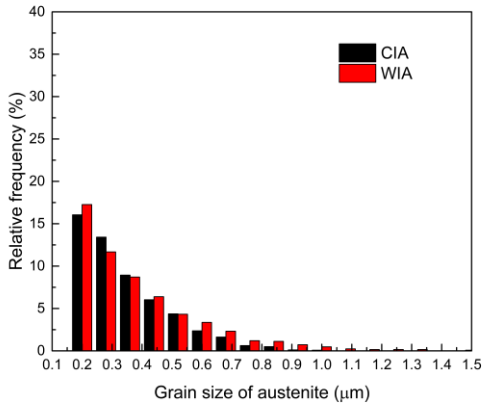

Figure 7. EBSD data: distribution of retained austenite grain size of CIA (black bar) and WIA (red bar), respectively.

Table 1 Tensile properties of 9Mn steels after different rolling process and treatment

Process	YS/MPa	UTS/MPa	TE/%	UTS× TE (GPA%)
WIA	989	1418	30	42.54
CIA	936	1438	21	30.20

According to TEM observation (see figure 4), we also find lamellar austenite and ferrite except for microstructure like CIA, which is attributed to relatively weak recrystallization behavior of ferrite or martensite. It has been reported that lamellar austenite has higher mechanical stability than equiaxed one because large interface and short diffusion path led to high content of carbon 18. Hence, the lamellar austenite with high stability would be motivated at the later of stage 3st, providing great work hardening and resulting in a flat work hardening behavior. In summary, duplex morphologies and wide size distribution of austenite in WIA contribute to a wider range of TRIP-related work hardening behavior, leading to the highest combination of UTS and TE.

4 CONCLUSION

In this paper, we investigated the microstructure evolution during cold rolling, warm rolling and subsequent intercritical annealing, and corresponding mechanical properties. The work hardening behaviors and austenite stability were also discussed. The main conclusions and findings are as following:

1) A higher recrystallization behavior is obtained in CIA sample than WIA sample, affecting the growth mechanism of austenite. For CIA, austenite nucleated at the recrystallized ferrite grain boundaries would grow to an equiaxed morphology. For WIA, except the equiaxed austenite, austenite nucleated at the lamellar ferrite boundaries would grow along the boundaries resulting in lamellar morphology.

2) The work hardening behaviors of both CIA and WIA samples exhibit significantly fluctuating which is attributed to the discontinuous TRIP. The lamellar austenite with higher stability is found in WIA. Multi-scale of size distribution and duplex morphologies of austenite in WIA result in more sustainable work hardening and the highest combination of UTS and TE.

Acknowledgments

This work was financially supported by the National Natural Science Foundation of China (NO. 51775102), and National Key R&D Program of China (2017YFB0703001 and 2018YFB1308704).

REFERENCES

1 Haldar A, Suwas S, Bhattacharjee D. Microstructure and Texture in Steels. London: Springer, 2009.

2 E. De Moor, P.J. Gibbs, J.G. Speer, D.K. Matlock, and J.G. Schroth: Iron Steel Technol, 2010; 7: 132-44.

3 Hu B, Luo H, Yang F, et al. Recent progress in medium-Mn steels made with new designing strategies, a review. Journal of Materials Science & Technology, 2017: S1005030217301688.

4 Gibbs P J , Moor E D , Merwin M J , et al. Austenite Stability Effects on Tensile Behavior of Manganese-Enriched-Austenite Transformation-Induced Plasticity Steel. Metallurgical & Materials Transactions A, 2011; 42(12):3691-3702.

5 Xiong X C , Chen B , Huang M X , et al. The effect of morphology on the stability of retained austenite in a quenched and partitioned steel. Scripta Materialia, 2013; 68(5):321-324.

6 Shao C , Hui W , Zhang Y , et al. Microstructure and mechanical properties of hot-rolled medium-Mn steel containing 3% aluminum. Materials Science & Engineering A, 2017; 682:45-53.

7 Lee YK, Han J. Current opinion in medium manganese steel. Mat Sci Tech. 2014; 31(7): 843–856.

8 Bin H , Haiwen L . Microstructures and Mechanical Properties of 7Mn Steel Manufactured by Different Rolling Processes. Metals, 2017; 7(11):464.

9 Magalhães A S , Dos Santos C E , Ferreira A O V , et al. Analysis of medium manganese steel through cold-rolling and intercritical annealing or warm-rolling. Materials Science and Technology, 2018:1-14.

10 Hu B , Luo H . A strong and ductile 7Mn steel manufactured by warm rolling and exhibiting both transformation and twinning induced plasticity. Journal of Alloys and Compounds, 2017; 725:684-693.

11 Li X , Song R , Zhou N , et al. An ultrahigh strength and enhanced ductility cold-rolled medium-Mn steel treated by intercritical annealing. Scripta Materialia, 2018; 154:30-33.

12 Shi J , Sun X , Wang M , et al. Enhanced work-hardening behavior and mechanical properties in ultrafine-grained steels with large-fractioned metastable austenite. Scripta Materialia, 2010; 63(8):815-818.

13 Conrad H . Effect of stress on the lüders band velocity in low carbon steels. Journal of the Mechanics & Physics of Solids, 1963; 11(6): 437-440.

14 Tsuchida N, Tomota Y, Nagal K, et al. A simple relationship between Lüders elongation and work-hardening rate at lower yield stress. Scripta Materialia, 2006; 54(1): 57-60.

15 Cai Z H , Ding H , Misra R D K , et al. Austenite stability and deformation behavior in a cold-rolled transformation-induced plasticity steel with medium manganese content. Acta Materialia, 2015; 84: 229-236.

16 J. Zrník, O. Muránsky, P. Luká, et al. Retained austenite stability investigation in TRIP steel using neutron diffraction. Materials Science & Engineering A, 2006; 437(1): 114-119.

17 Moor E D , Matlock D K , Speer J G , et al. Austenite stabilization through manganese enrichment. Scripta Materialia, 2011; 64(2): 185-188.

18 Park H S , Han J C , Lim N S , et al. Nano-scale observation on the transformation behavior and mechanical stability of individual retained austenite in CMnSiAl TRIP steels. Materials Science and Engineering: A, 2015; 627: 262-269.